Spectral Efficiency Analysis of Uplink-Downlink Decoupled Access in C-V2X Networks

PERFORMANCE MODELING FOR MOBILE COMMUNICATIONS NETWORKING SYSTEMS FINAL PROJECT

徐振宗
資工所碩一 r11922188

栗漢文
資工所碩一 r11922191

青光恆
資工所碩一 r11922120

Abstract—With the development of mobile networks, C-V2X applications are becoming more and more advanced. We studied a paper on how to establish an analysis model for C-V2X and simulated to reproduce the experimental results of this paper.

I. INTRODUCTION

3GPP Cellular V2X (C-V2X) is an innovative technology designed for transportation that allows cars to communicate with each other and even with surrounding devices. In order to improve the safety of drivers, passengers and pedestrians, C-V2X provides low-latency communication directly between general vehicles (V2V), roadside infrastructure (V2I), drivers and pedestrians (V2P), and cars to the network (V2N). Therefore, the quality of service (QoS) of the network is important for C-V2X applications.

Currently, C-V2X is gradually evolving into a more complex heterogeneous network composed of macro base stations (MBS) and small base stations (SBS). It is generally believed that users located at the edge of SBS choose to access SBS in uplink (UL) and MBS in downlink (DL), which can significantly improve the UL rate in heterogeneous networks in cellular networks. This is essential for high UL rate guarantees such as safety information sharing and remote driving in C-V2X.

Therefore, the paper we found studies the spectrum efficiency of UL and DL access to different base stations in C-V2X. It models UL/DL decoupling access to C-V2X as a Cox process and proposes a unified analytical framework. Through stochastic geometry, it provides in-depth theoretical analysis, including joint association probability, UL/DL distance distribution to service BS, and associated cases in C-V2X networks.

II. SYSTEM MODEL

The system model consists of the following five elements (Figure 1):

- The overall area of the system
- Macro Base Station (MBS)
- Road
- Small Base Station (SBS)
- Vehicle

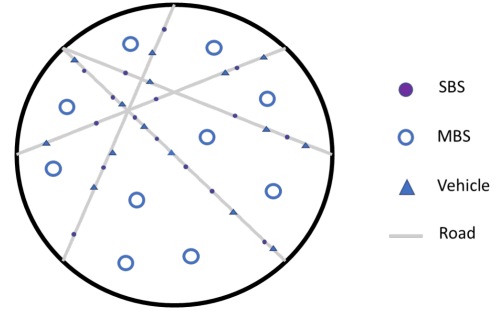1) The overall area of the system is set as a plane of a circle with a radius of R.

Fig. 1. Illustration of the system model

2) Macro Base Station (MBS) is evenly distributed in the circle and simulated using a 2D Poisson point process (PPP) with a density λ_m.

3) Roads are simulated by Poisson Line process (PLP). In the plane, lines can be transformed into a 1-to-1 transformation by taking the intersection of the perpendicular line from the origin to the line. And then transform the point into polar coordinates (Figure 2). Therefore, we can use 2D PPP to simulate PLP, and the density of PPP is λ_r.

4) Small Base Station (SBS) is simulated using a 1D PPP with density λ_s on each line generated by 3.

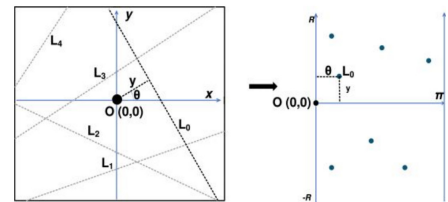5) Vehicle is simulated using a 1D PPP with a density λ_v on each line generated by 3.

Fig. 2. Illustration of a line converted into point [2]

A. Power Transmission

To analyze the transmission power between vehicles and base stations (BS) in this model, this paper defines the following transmission powers:

the DL transmit power can be written as

$$P_{r,V} = \begin{cases} P_M G_M H_M \chi_M \|x\|^{-\alpha_M}, & x \in \Phi_M \\ P_S G_{S,0} H_{S,0} \chi_{S,0} \|x\|^{-\alpha_S}, & x \in \Xi_{l_0}^{(S)} \\ P_S G_{S,1} H_{S,1} \chi_{S,1} \|x\|^{-\alpha_S}, & x \in \Phi_S \backslash \Xi_{l_0}^{(S)}, \end{cases}$$

the UL transmit power can be written as

$$P_{r,M} = P_V G_{V,1} H_{V,1} \chi_M \|x\|^{-\alpha_M}, \quad x \in \Phi_M,$$

$$P_{r,S} = \begin{cases} P_V G_{V,0} H_{V,0} \chi_{S,0} \|x\|^{-\alpha_S}, & x \in \Xi_{l_0}^{(S)} \\ P_V G_{V,1} H_{V,1} \chi_{S,1} \|x\|^{-\alpha_S}, & x \in \Phi_S \backslash \Xi_{l_0}^{(S)}, \end{cases}$$

and the definition of parameters above are as follows.

Φ_M : the set of MBSs

Φ_S : the set of SBSs

$\Xi_{l_0}^{(S)}$: the set of SBSs in the typical line

P : transmit power

G : antenna gains

H : channel fading gains

χ : shadowing effects

x : distance between vehicle and BS

α : power-law loss parameters

These three power measurements are further categorized into different cases based on the type of base station. The Figure 3 shows the cases in different base station applied scenarios.
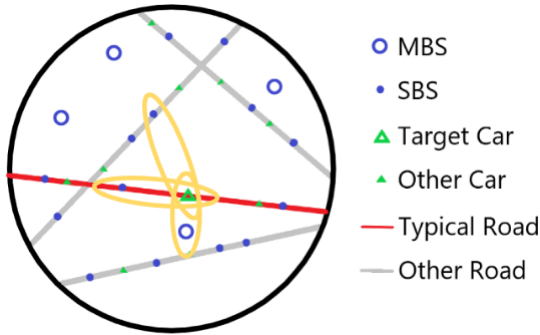

Fig. 3. Power transmission between different base station

B. Power Transmission Cases

For the convenience of analysis, this paper divides the cases based on the base stations (BS) connected to the downlink (DL) and uplink (UL) into four categories as follows.

 – Case 1: UL = MBS, DL = MBS
 – Case 2: UL = SBS, DL = MBS
 – Case 3: UL = MBS, DL = SBS
 – Case 4: UL = SBS, DL = SBS

III. SPECTRAL EFFICIENCY ANALYSIS

We assume that a vehicle is associated with the MBS/SBS which yields the highest biased received power in DL, similarly,the MBS/SBS will serve the vehicle with the highest transmit power in UL, namely the vehicles in the Voronoi cell of a BS connect to it.

Spectral efficiency refers to the amount of data that can be transmitted over a given bandwidth. In this paper, summing up the data rates in different cases yields our Spectral Efficiency.

A. Distance Distribution

we first need to compute the distance distribution between the vehicle and the BS. the cumulative distribution functions (CDF) of x_S, x_M are

$$F_S(x_S) = 1 - \exp(-2\lambda_S x_S)$$
$$F_S(x_S) = 1 - \exp(-\lambda_M \pi x_S^2) \tag{1}$$

According to $f(x) = dF(x)/dx$, the probability density functions (PDF) of x_S, x_M are

$$f_S(x_S) = 2\lambda_S \exp(-2\lambda_S x_S)$$
$$f_M(x_M) = 2\pi x_M \lambda_M \exp(-\lambda_M \pi x_M^2) \tag{2}$$

B. Joint Association Probability

Since both UL and DL are connected to MBS in Case 1, we can derive the following formula:

$$P_M G_M B_M \|x_M\|^{-\alpha_M} > P_S G_{S,0} B_S \|x_S\|^{-\alpha_S}$$
$$P_V G_{V,1} \|x_M\|^{-\alpha_M} > P_V G_{V,0} \|x_S\|^{-\alpha_S} \tag{3}$$

We denote

$$A_{M,S} = P_M G_M B_M / P_s G_{s,0} B_s$$
$$B_{M,S} = P_V G_{V,1} / P_V G_{V,0} \tag{4}$$

Substituting for (3) :

$$A_{M,S} \|x_M\|^{-\alpha_M} > \|x_S\|^{-\alpha_S},$$
$$B_{M,S} \|x_M\|^{-\alpha_M} > \|x_S\|^{-\alpha_S}, \tag{5}$$

Furthermore, since the transmit power of MBS is much larger than that of SBS and vehicle, we can assume that $A_{M,S} > B_{M,S}$.So the joint probability of Case 1 can be written as:

$$\Pr(\text{Case1}) = \Pr(A_{M,S} X_M^{-\alpha_M} > X_S^{-\alpha_S}; B_{M,S} X_M^{-\alpha_M} > X_S^{-\alpha_S})$$
$$= \Pr\left(B_{M,S} X_M^{-\alpha_M} > X_S^{-\alpha_S}\right)$$
$$= E_{X_S}\left[\Pr\left(X_M < B_{M,S}^{\frac{1}{\alpha_M}} x_S^{\frac{\alpha_S}{\alpha_M}} \mid X_S\right)\right]$$
$$= \int_0^\infty F_M\left(B_{M,S}^{\frac{1}{\alpha_M}} x_S^{\frac{\alpha_S}{\alpha_M}}\right) f_S(x_S) \, dx_S$$
$$= 1 - \int_0^\infty \left[2\lambda_S \exp\left(-\lambda_M \pi B_{M,S}^{\frac{2}{\alpha_M}} x_S^{\frac{2\alpha_S}{\alpha_M}} - 2\lambda_S x_S\right)\right] dx_S, \tag{6}$$

Since x_S and x_M are both random variables, we can consider this as the summation of the probability that x_M satisfies the

condition for different x_S. Then, by applying the derived CDF and PDF formulas for distance, we can obtain the probability of each case occurring.

$$\Pr(\text{ Case 2}) = \Pr\left(A_{M,S}X_M^{-\alpha_M} > X_S^{-\alpha_S}; \right.$$
$$\left. B_{M,S}X_M^{-\alpha_M} < X_S^{-\alpha_S}\right) \quad (7)$$
$$= \Pr\left(B_{M,S}X_M^{-\alpha_M} < X_S^{-\alpha_S} < A_{M,S}X_M^{-\alpha_M}\right)$$

$$\Pr(\text{ Case 3}) = \Pr\left(A_{M,S}X_M^{-\alpha_M} < X_S^{-\alpha_S}; \right.$$
$$\left. B_{M,S}X_M^{-\alpha_M} > X_S^{-\alpha_S}\right) \quad (8)$$

$$\Pr(\text{ Case 4}) = \Pr\left(A_{M,S}X_M^{-\alpha_M} < X_S^{-\alpha_S}; \right.$$
$$\left. B_{M,S}X_M^{-\alpha_M} < X_S^{-\alpha_S}\right) \quad (9)$$
$$= \Pr\left(X_S < A_{S,M}^{\frac{1}{\alpha_S}}X_M^{\frac{\alpha_M}{\alpha_S}}\right)$$

It is worth noting that in Case 3, since we assume that $A_{M,S}$ is greater than $B_{M,S}$, the scenario where DL is SBS and UL is MBS will not occur.

C. Distance Distribution of A Vehicle to Serving BSs

Next, we need to calculate the PDF of the distance between each vehicle and BS under different cases. The core calculation method is to first calculate the CCDF of x_S under a specific case, then obtain its CDF through $1 - CCDF$, and finally differentiate CDF to obtain the PDF.

$$f_{X_M|\text{ Case 1}} = \frac{\exp\left(-\lambda_S\pi 2B_{S,M}^{\frac{1}{\alpha_S}}x^{\frac{\alpha_M}{\alpha_S}}\right)f_{X_M}(x)}{\Pr(\text{ Case 1})}$$

$$f_{X_M|\text{ Case 2}} = \frac{f_{X_M}(x)}{\Pr(\text{ Case 2})}\left[\exp\left(-\lambda_S\pi 2A_{S,M}^{\frac{1}{\alpha_S}}x^{\frac{\alpha_M}{\alpha_S}}\right) - \right.$$
$$\left. \exp\left(-\lambda_S\pi 2B_{S,M}^{\frac{1}{\alpha_S}}x^{\frac{\alpha_M}{\alpha_S}}\right)\right]$$

$$f_{X_S|\text{ Case 2}} = \frac{f_{X_S}(x)}{\Pr(\text{ Case 2})}\left[\exp\left(-\lambda_M\pi B_{M,S}^{\frac{2}{\alpha_M}}x^{\frac{\alpha_S}{\alpha_M}}\right) - \right.$$
$$\left. \exp\left(-\lambda_M\pi A_{M,S}^{\frac{2}{\alpha_M}}x^{\frac{\alpha_S}{\alpha_M}}\right)\right]$$

$$f_{X_S|\text{ Case 4}} = \frac{\exp\left(-\lambda_M\pi A_{M,S}^{\frac{2}{\alpha_M}}x^{\frac{2\alpha_S}{\alpha_M}}\right)f_{X_S}(x)}{\Pr(\text{ Case 4})}$$

$$(10)$$

D. Spectral Efficiency

$$SE = \sum_{i=1}^{4}\sum_{n}^{\{U,D\}}\tau_{\text{Case } i}^n\Pr(\text{ Case } i), \quad (11)$$

Our goal is to calculate the overall spectral efficiency. To do this, we have previously calculated the probability of each case occurring. Now, we need to calculate the data rate under each case.

Here, the $\ln\left(1 + SINR_{U,S}\right)$ refers to Shannon capacity, which is used to calculate the data rate. Take Case 2 as example, this formula calculates the expected value of the data rate under different cases. $f_{S|2}$ represents the probability of the distance between SBS and vehicles under Case 2. The inner integral calculates the expected value of the data rate under that distance. The data rate for the other cases can also be calculated using a similar method.

$$\tau_2^U = E\left[\ln\left(1 + SINR_{U,S}\right)\right]$$
$$= \int_0^\infty f_{S|2}\int_0^\infty \Pr\left[\ln\left(1 + \frac{P(X^*)}{I_{U,2}}\right) > t\right]dtdx_S$$
$$= \int_0^\infty f_{S|2}\int_0^\infty \Pr\left[H_{V,0} > \frac{(e^t - 1)I_{U,2}}{P_V G_{V,0}}x_S^{\alpha_S}\right]dtdx_S$$
$$\overset{(a)}{=} \int_0^\infty f_{S|2}\int_0^\infty \Pr\left[H_{V,0} > \beta_{S,0}I_{U,2}x_S^{\alpha_S}\right]dtdx_S,$$
$$\tau_2^D = E\left[\ln\left(1 + SINR_{D,M}\right)\right]$$
$$= \int_0^\infty f_{M|2}\int_0^\infty \Pr\left[H_M > \frac{(e^t - 1)I_{D,3}}{P_M G_M}x_M^{a_M}\right]dt\ dx_M$$
$$(12)$$

$$\tau_1^U = \int_0^\infty f_{M11}\int_0^\infty \Pr\left[H_{v,1} > \frac{(e^t - 1)I_{U,2}}{P_v G_{v,1}}x_M^{\alpha_M}\right]dt\ dx_M$$
$$\tau_1^D = \int_0^\infty f_{M|1}\int_0^\infty \Pr\left[H_M > \frac{(e' - 1)I_{D,3}}{P_M G_M}x_M^\alpha\right]dt\ dx_M$$
$$(13)$$

$$\tau_4^U = \int_0^\infty f_{S|4}\int_0^\infty \Pr\left[H_{v,0} > \frac{(e^i - 1)I_{U,2}}{P_v G_{v,0}}x_s^{\alpha_s}\right]dt\ dx_s$$
$$\tau_4^D = \int_0^\infty f_{s|4}\int_0^\infty \Pr\left[H_{s,0} > \frac{(e^t - 1)I_{D,3}}{P_{s,0}G_{s,0}}x_s^{\alpha_s}\right]dt\ dx_s$$
$$(14)$$

IV. SIMULATION

A. Numerical Results

This paper presents numerical results in the form of two charts:

1) Joint probability of association Figure 4
2) Spectral efficiency. Figure 5

B. SE simulation algorithm

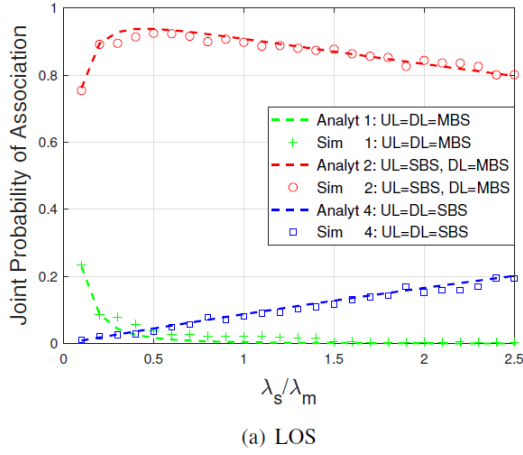The algorithm for simulating decoupled spectral efficiency is as Algorithm 1.

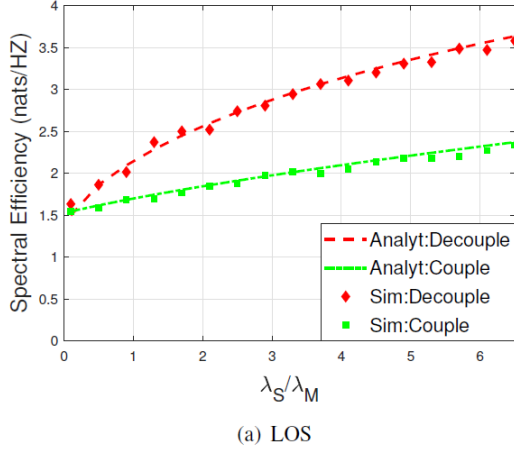Fig. 4. Joint probability of association (LOS)

Fig. 5. Spectral Efficiency(nats/HZ) (LOS)

Algorithm 1 Spectral Efficiency Monte Carol Simulation

1: $r \leftarrow 5$ (radius)
2: $monte \leftarrow 10$ (Monte Carol iterations)
3:
4: **for** $\lambda_S/\lambda_M \leftarrow 0.1$ to 6.5 **do**
5:     **for** $m \leftarrow 1$ to $monte$ **do**
6:         1. Sample the number of MBSs, SBSs and vehicles from Poisson
7:         2. Distributing MBSs, SBSs and vehicles
8:         **for** $v \leftarrow 1$ to number of vehicles **do**
9:             3. Find BS (DL and UL) that delivers maximum power for v
10:             4. Compute SINR and SE
11:             5. Assign a case label to v
12:         **end for**
13:         6. Compute avg. SE for each case
14:         7. Compute avg. SE across all cases
15:     **end for**
16:     8. Compute avg. SE across all simulation iteration
17: **end for**

C. Our Simulation

The figures Figure 6 Figure 7 Figure 8 Figure 9 shows our works.
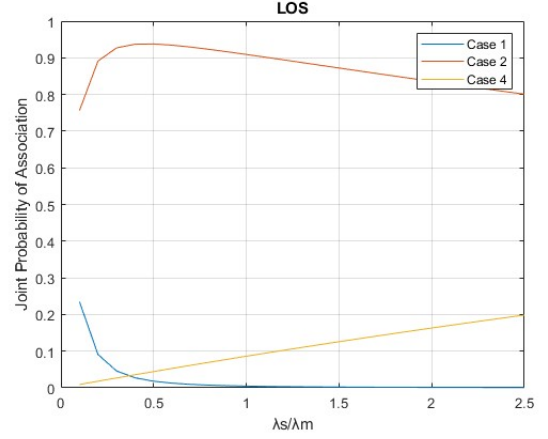
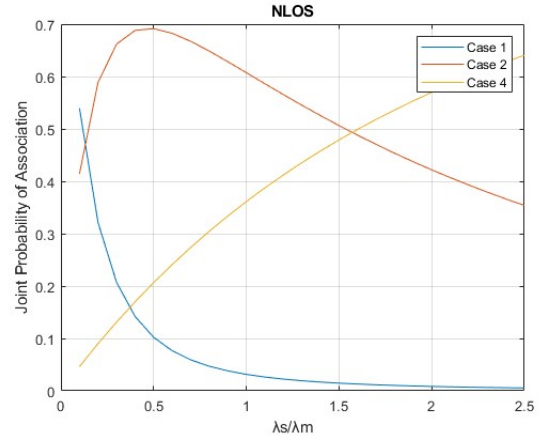

Fig. 6. Our Joint probability of association (LOS)

Fig. 7. Our Joint probability of association (NLOS)

D. Conclusion

Our simulation results closely align with the results of the original paper, indicating that our modeling approach is correct.

The experiment presents that the line-of-sight (LOS) spectral efficiency have a significant improvement in the decoupled scenario. The original authors analyzed this phenomenon and attributed it to an increased proportion of small base stations (SBS) being used for uplink (UL) transmission. As the density of SBS increases, vehicles are closer to SBS, resulting in better UL power compared to macro base stations (MBS). Consequently, the increased proportion of SBS being used for UL transmission leads to a significant improvement in spectral efficiency.

In the future, we may considering applying this modeling approach to other application scenarios.
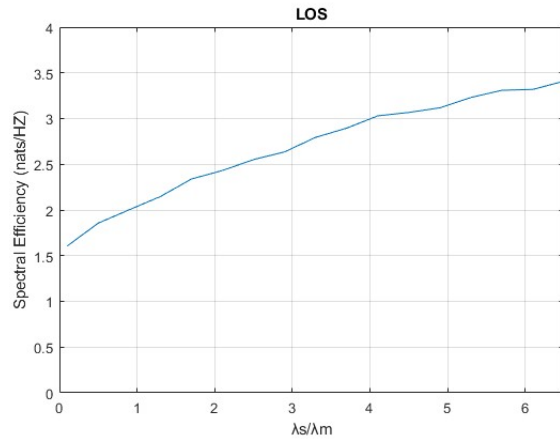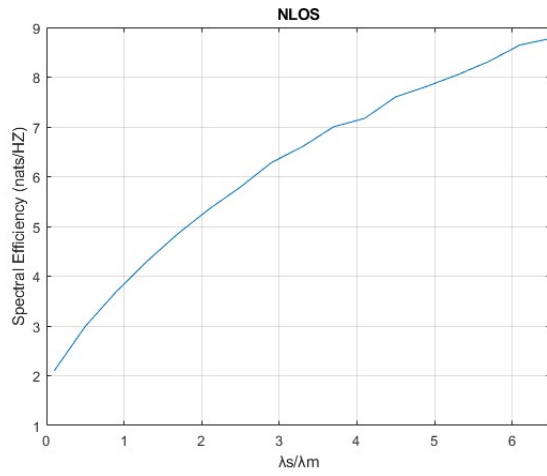
Fig. 8. Our Spectral Efficiency Simulation(LOS)

Fig. 9. Our Spectral Efficiency Simulation(NLOS)

REFERENCES

[1] Luofang Jiao, Kai Yu, Yunting Xu, Tianqi Zhang, Haibo Zhou, and Xuemin (Sherman) Shen.,"Spectral Efficiency Analysis of Uplink-Downlink Decoupled Access in C-V2X Networks" in 2022 IEEE Global Communications Conference

[2] M. N. Sial, Y. Deng, J. Ahmed, A. Nallanathan and M. Dohler, "Stochastic Geometry Modeling of Cellular V2X Communication Over Shared Channels," in IEEE Transactions on Vehicular Technology, vol. 68, no. 12, pp. 11873-11887, Dec. 2019, doi: 10.1109/TVT.2019.2945481.

[3] Z. Sattar, J. V. Evangelista, G. Kaddoum, and N. Batani, "Spectral efficiency analysis of the decoupled access for downlink and uplink in two-tier network," IEEE Transactions on Vehicular Technology, vol. 68, no. 5, pp. 4871–4883, 2019.

[4] Chetlur, Vishnu Vardhan and Dhillon, Harpreet S, "Coverage and rate analysis of downlink cellular vehicle-toeverything (C-V2X) communication," IEEE Transactions on Wireless Communications, vol. 19, no. 3, pp. 1738– 1753, 2019.